

An analysis of the automotive driveline dynamic behaviour focusing on the influence of the oil squeeze effect on the idle rattle phenomenon

Renato Brancati, Ernesto Rocca, Riccardo Russo*

Dipartimento di Ingegneria Meccanica per l'Energetica, Università di Napoli "Federico II", via Claudio, 21 80125 Napoli, Italy

Received 3 April 2006; received in revised form 31 January 2007; accepted 6 February 2007

Available online 29 March 2007

Abstract

In this paper a theoretical analysis concerning the influence of the oil damping effects on the dynamic behaviour of manual automotive transmissions, in the “idle” operating condition, is proposed. The study presents an analytical model that accounts both for the hysteretic friction in the clutch springs and for the oil squeeze effect between the impacting teeth of the meshing gears. This last dissipative term, generally neglected in the literature, has been modelled by the authors in order to consider its influence on the “gear rattle” phenomenon. The results provided by a wide numerical investigation are presented and enable a qualitative comparison between the effects due to the oil and those due to the hysteretic friction in the clutch on the rattle level.

© 2007 Elsevier Ltd. All rights reserved.

1. Introduction

The noise inducted by the vibrations among the unloaded gears of automotive transmissions is of great interest to car designers. The phenomenon, known as “gear rattle noise”, is particularly audible at low speed regimes of the engine and is generated by the irregularity of the I.C. engine torque, causing impacts between the teeth of all the gears that are in meshing but without loading, due to the presence of backlashes.

In recent years, many solutions have been proposed that aim either to reduce the noise or eliminate its occurrence using some devices as multi-stage clutches or dual mass flywheels.

The clutch is a component of the driveline that can play a significant role on the vibrations of the gear pairs filtering out the internal combustion engine velocity fluctuations. Gear rattle noise can be greatly reduced by opportunely setting some clutch parameters such as the multi-stage torsional springs. In order to reduce the negative effects of the I.C. engine irregularities on the driveline it is also possible to adopt a dual mass flywheel (DMF). This component gives a great contribution to the vibration isolation of the system filtering out engine irregularity, and making the operation of the secondary flywheel side almost uniform, and thus also of the

*Corresponding author. Tel.: +39 0817683292; fax: +39 0812394165.

E-mail address: riccardo.russo@unina.it (R. Russo).

transmission input shaft. By contrast due to complexity and high costs, the DMF at present can be applied only to high class vehicles.

Another possibility is offered by the lubricant oil. The presence of a drop of oil between the impacting teeth may provide a damping force useful to reduce the effects of the impact. This oil factor is still poorly understood and an analytical formulation of the problem could be useful in order to evaluate its influence.

In the scientific literature several theoretical analyses based on nonlinear models have been proposed to investigate the vibrations of automotive transmissions [1–6]. The models adopted are torsional models describing the dynamic behaviour of the driveline components. The complexity of the models is generally due to the presence of many mechanical components such as flywheel, clutch, gears, bearings, springs, that introduce into the system several nonlinear effects due to the meshing stiffness, to the gear backlashes, to the springs friction hysteresis, and so on.

A dynamic analysis of the automotive driveline can be conducted adopting a nonlinear “uncoupled” model in order to simplify the study [4]. Using this approach, the torsional loaded path can be separated from the unloaded gear pairs. Firstly, the driveline torsional analysis must be conducted on the loaded baseline path and, successively, every pair of unsynchronized gears can be simply modelled as a single d.o.f. system, where the excitation is that previously obtained in the baseline torsional study.

Following another approach the dynamic behaviour of the driveline can be analysed through a complete “coupled” model that considers the contemporary interactions between the loaded and unloaded system components [1,5,6].

The clutch capability in reducing gear rattle noise has been theoretically investigated with reference to the influence on the phenomenon exerted by some clutch parameters, such as the multi-stage torsional springs [1,4]. Moreover, by accounting for the torsional spring hysteresis an effect on the dynamic behaviour of the driveline has been noted [3,5].

A theoretical analysis on the influence of the dual mass flywheel has been also developed [7].

In the literature, it is possible to find some numerical studies that adopt techniques based on multi-body codes or on finite element methods. These numerical methods are useful particularly for the automotive industries because they make it possible to quickly analyse the influence of a particular mechanical parameter or of a particular design option on the dynamic behaviour of the entire power-train, accounting also for the gear rattle in the unloaded gear pairs [8–10].

Finally, experimental studies conducted mainly to evaluate and to optimize the noise effects of the gear rattle on the transmissions, have been recently published [11–13], but a correlation with the theoretical predictions of the dynamic behaviour in terms of gear impacts and vibrations, seems, at present, not still available.

The present paper falls within the theoretical studies, and proposes a driveline dynamic analysis focusing on the influence of some dissipative terms on the gear rattle phenomenon, with a particular attention to the oil damping between the impacting teeth.

In a previous paper [14], with reference to a single unloaded gear pair, the authors investigated on the rattle noise reduction due to the oil between the teeth. The drag torque exerted on the unloaded gears by the oil between the impacting teeth depends primary on its quantity and viscosity, and can be, in some cases, not negligible.

The theoretical model adopted in the present paper is a complete “coupled” model and is composed by constant inertia parameters such as the flywheel, the input and the output gear inertial elements, each characterized by a torsional displacement.

The clutch is modelled in terms of torque vs. relative angular displacement, accounting also for the spring hysteresis. The various shaft elements connecting the gears are modelled by linear torsional springs and dampers. The interfacial contact between the gears is described by mesh stiffness [15,16] with the presence, during the crossing of the “dead space” representing the teeth backlash, of a damping term due to the oil squeezed between the teeth.

2. The driveline model

The considered system is constituted by a flywheel, a clutch and the gear pairs of an automotive gear box at “idle” operating conditions. Therefore, no load is applied to the output shaft of the gear box.

The gear box under examination is characterized by the pinions of the first and second gears fitted on the primary shaft, while those of the other gear pairs are fitted on the secondary shaft and, therefore, under the hypothesis of “idle” operating conditions they do not rotate. Under these conditions the only wheels involved in the gear rattle phenomenon are the driven ones of the first and second speeds.

The engine torque applied to the flywheel is then transmitted through the clutch to the primary shaft and therefore to the two pinions of the first and second gears.

The motion of the two driven gears is constrained only by the mechanical losses in the two bearings with which they are coupled to the secondary shaft.

The lumped parameters physical model of the system, Fig. 1, is constituted by five inertia terms: the flywheel, the four wheels of the two gear pairs, i.e. the first and second speed. The clutch mass is neglected.

The flywheel is connected to the first gear shift pinion by a nonlinear term that models the clutch stiffness and damping, while the pinion of the first speed is coupled to the second one by two linear stiffness and damping terms representing the shaft section that separates them. Finally, between the meshing teeth of the two gears either the contact forces and the squeeze forces representing the actions exerted by the oil during the no-contact phase are present.

Indicating with $I_f, I_{1P}, I_{2P}, I_{1S}, I_{2S}$ the constant inertia terms, $T_e(t)$ the engine torque, with K_t, σ_t the primary shaft torsional stiffness and damping coefficients, with T_{b1}, T_{b2} the two constant drag torques representing the losses in the bearings supporting the driven gears on the secondary shaft, the mathematical model is

$$\begin{aligned}
 & -I_f \ddot{\vartheta}_f - T_c[(\dot{\vartheta}_f - \dot{\vartheta}_{1P}), (\vartheta_f - \vartheta_{1P})] + T_e[t] = 0, \\
 & -I_{1P} \ddot{\vartheta}_{1P} + T_c[(\dot{\vartheta}_f - \dot{\vartheta}_{1P}), (\vartheta_f - \vartheta_{1P})] - \sigma_t(\dot{\vartheta}_{1P} - \dot{\vartheta}_{2P}) - K_t(\vartheta_{1P} - \vartheta_{2P}) - F_{c1}[\vartheta_{1P}, \vartheta_{1S}, (\dot{\vartheta}_{1P} - \dot{\vartheta}_{1S})]r_{1P} = 0, \\
 & -I_{2P} \ddot{\vartheta}_{2P} - \sigma_t(\dot{\vartheta}_{2P} - \dot{\vartheta}_{1P}) - K_t(\vartheta_{2P} - \vartheta_{1P}) - F_{c2}[\vartheta_{2P}, \vartheta_{2S}, (\dot{\vartheta}_{2P} - \dot{\vartheta}_{2S})]r_{2P} = 0, \\
 & -I_{1S} \ddot{\vartheta}_{1S} + F_{c1}[\vartheta_{1P}, \vartheta_{1S}, (\dot{\vartheta}_{1P} - \dot{\vartheta}_{1S})]r_{1S} - T_{b1} = 0, \\
 & -I_{2S} \ddot{\vartheta}_{2S} + F_{c2}[\vartheta_{2P}, \vartheta_{2S}, (\dot{\vartheta}_{2P} - \dot{\vartheta}_{2S})]r_{2S} - T_{b2} = 0,
 \end{aligned}
 \tag{1}$$

where $r_{1P}, r_{2P}, r_{1S}, r_{2S}$ are the base radii of the involute tooth pairs.

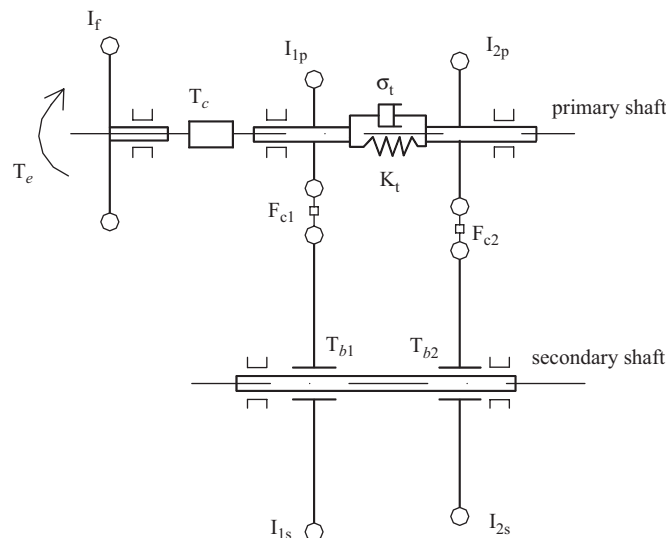


Fig. 1. Drive line scheme at “idle” operating conditions.

Due to the following congruence conditions:

$$\begin{aligned} \vartheta_{1S} &= \vartheta_{1P} \frac{r_{1P}}{r_{1S}} + \Delta\vartheta_1, \\ \vartheta_{2S} &= \vartheta_{2P} \frac{r_{2P}}{r_{2S}} + \Delta\vartheta_2, \end{aligned} \tag{2}$$

Eq. (1) can be rewritten as

$$\begin{aligned} -I_f \ddot{\vartheta}_f - T_c[(\dot{\vartheta}_v - \dot{\vartheta}_{1P}), (\vartheta_v - \vartheta_{1P})] + T_e[t] &= 0, \\ -I_{1P} \ddot{\vartheta}_{1P} + T_c[(\dot{\vartheta}_v - \dot{\vartheta}_{1P}), (\vartheta_v - \vartheta_{1P})] - \sigma_t(\dot{\vartheta}_{1P} - \dot{\vartheta}_{2P}) - K_t(\vartheta_{1P} - \vartheta_{2P}) - F_{c1}[\vartheta_{1P}, \Delta\vartheta_1, \Delta\dot{\vartheta}_1]r_{1P} &= 0, \\ -I_{2P} \ddot{\vartheta}_{2P} - \sigma_t(\dot{\vartheta}_{2P} - \dot{\vartheta}_{1P}) - K_t(\vartheta_{2P} - \vartheta_{1P}) - F_{c2}[\vartheta_{2P}, \Delta\vartheta_2, \Delta\dot{\vartheta}_2]r_{2P} &= 0, \\ -I_{1S} \Delta \ddot{\vartheta}_1 + F_{c1}[\vartheta_{1P}, \Delta\vartheta_1, \Delta\dot{\vartheta}_1]r_{1S} - T_{b1} - I_{1S} \ddot{\vartheta}_{1P} \frac{r_{1P}}{r_{1S}} &= 0, \\ -I_{2S} \Delta \ddot{\vartheta}_2 + F_{c2}[\vartheta_{2P}, \Delta\vartheta_2, \Delta\dot{\vartheta}_2]r_{2S} - T_{b2} - I_{2S} \ddot{\vartheta}_{2P} \frac{r_{2P}}{r_{2S}} &= 0. \end{aligned} \tag{3}$$

A particular attention is necessary to describe the torque $T_c[(\dot{\vartheta}_f - \dot{\vartheta}_{1P}), (\vartheta_f - \vartheta_{1P})]$ representing the clutch, and the interaction forces $F_{c1}[\vartheta_{1P}, \Delta\vartheta_1, \Delta\dot{\vartheta}_1]$, $F_{c2}[\vartheta_{2P}, \Delta\vartheta_2, \Delta\dot{\vartheta}_2]$ exerted among the teeth of the two gear pairs.

3. The clutch model

The adopted clutch model, due to Kim and Singh [5], includes a two-stage stiffness with an hysteretic behaviour.

Indicating with $\vartheta_c = \vartheta_f - \vartheta_{1P}$, the relative displacement between the flywheel and the first pinion of the gear box, such a model returns for the clutch torque the following expression:

$$\begin{aligned} T_c(\vartheta_c, \dot{\vartheta}_c) &= k_{c2}\vartheta_c + 0.5(k_{c2} - k_{c1})[(\vartheta_c - \phi)\xi(\vartheta_c - \phi, \sigma) - (\vartheta_c + \phi)\xi(\vartheta_c + \phi, \sigma)] + 0.5\xi(\dot{\vartheta}_c, \sigma)H_2 \\ &+ 0.25(H_2 - H_1)[(\xi(\vartheta_c + \phi, \sigma)(1 - \xi(\dot{\vartheta}_c, \sigma)) + \xi(\vartheta_c - \phi, \sigma)(1 - \xi(\dot{\vartheta}_c, \sigma))], \end{aligned} \tag{4}$$

in which the function $\xi(x, \sigma) = 2/\pi \arctan(\sigma x)$, replaces the $\text{sign}(x)$ function eliminating its discontinuity at $x = 0$ (normally $\sigma = 10^6$). In Eq. (4) ϕ is a transition angle, k_{c1} is the first stage stiffness and k_{c2} is the second stage stiffness.

The meaning of the hysteresis parameters H_1 and H_2 is shown in Fig. 2.

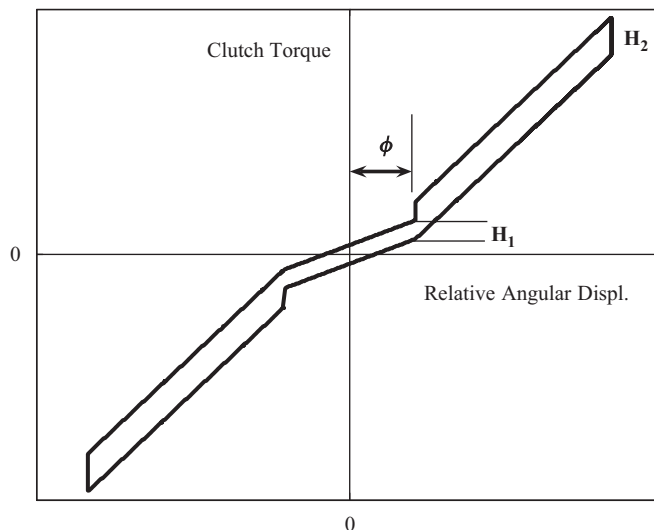


Fig. 2. Dual stage clutch characteristics.

4. The teeth contact model with oil squeeze

The generic interaction force F_c between the teeth is expressed as:

$$F_c(\vartheta_P, \Delta\vartheta, \Delta\dot{\vartheta}) = \begin{cases} K(\vartheta_P)r_S\Delta\vartheta, & \text{if } |r_S\Delta\vartheta| \geq b, \\ S(\Delta\vartheta)r_S\Delta\dot{\vartheta}, & \text{if } |r_S\Delta\vartheta| \leq (b - h_{\min}), \\ S_{\max}r_S\Delta\dot{\vartheta}, & \text{if } (b - h_{\min}) < |r_S\Delta\vartheta| < b, \end{cases} \quad (5)$$

where it has been assumed that the relative angular displacement $\Delta\theta$ is equal to 0 when the tooth of the secondary gear is just in the centre of the gap between the teeth of the primary gear (Fig. 3). In such condition the distance between the flanks of the teeth is indicated with b . Therefore, the instantaneous value of the distance between the approaching teeth is

$$\begin{cases} b - \Delta\vartheta r_s & \text{if } \Delta\dot{\vartheta} > 0, \\ b + \Delta\vartheta r_s & \text{if } \Delta\dot{\vartheta} < 0. \end{cases}$$

The minimum oil film thickness is denoted with h_{\min} . Assuming that during the contact phase an elastohydrodynamic lubrication regime is established, the h_{\min} value can be fixed almost equal to the average roughness R_a of the tooth flanks surfaces.

Therefore, when the distance between the flanks is less or equal to 0 the meshing stiffness $K(\theta_p)$, due to the elastic deformation of the teeth in contact, takes place, instead when the distance is greater then h_{\min} the term $S(\Delta\theta)$ representing the effect due to the oil film between the teeth, acts as a damping. Finally when the distance is positive but less then h_{\min} , the above damping term is assumed to be constant and equal to a saturation value: $S_{\max} = S(b - h_{\min})/r_s$.

5. The contact model

With reference to a helical involute gear pair, the contact stiffness $K(\vartheta_P)$ is given by the sum of the contributes due to the n tooth pairs that are in contact at the same time (Fig. 4).

According to other authors [4,15,16] this stiffness, for a given gear pair, is only function of the position of the driving gear during the meshing.

As an example in Fig. 4 the stiffness function of a gear pair characterized by a total contact ratio of 2.93, is reported.

The stiffness is consequently the sum of n periodic functions shifted each other of a transverse base pitch (Θ_P). Following Cai [16] the j th function $K_j(\vartheta_P)$ has the expression:

$$K_j(\vartheta_P) = k_p \exp\left(C_a \left| \frac{\vartheta_P - \varepsilon\Theta_P/2}{1.125\varepsilon_x\Theta_P} \right|^3\right) \quad (6)$$

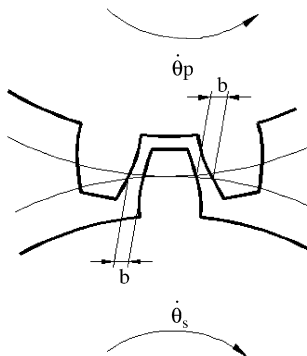


Fig. 3. The gears position for $\Delta\theta = 0$.

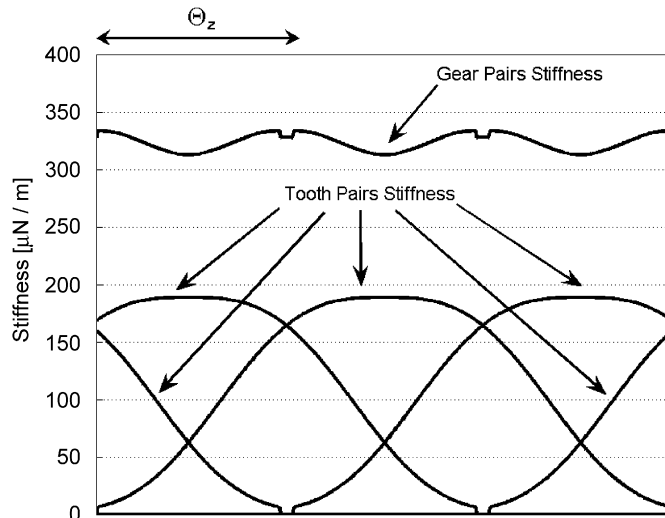


Fig. 4. The gear pair stiffness function.

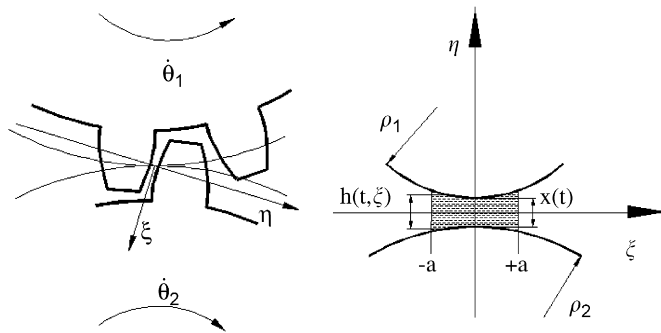


Fig. 5. The reference frame for the oil squeeze model.

where ε and ε_z are the total contact ratio and the transverse contact ratio respectively, and Θ_P is the transverse base pitch. In a complete meshing cycle, ϑ_P starts from 0 and ends at $\varepsilon\Theta_P$. With k_p is indicated the stiffness at the pitch point, that depends on the tooth parameters along with the C_a coefficient. These terms are detailed in [16].

6. The oil squeeze model

During the phase in which the teeth are not in contact, a damping force exerted by the oil film in the gap exists. Such force, in the authors knowledge, is neglected in the specific literature. In this paper a squeeze model developed by the authors [14] is included in the motion equation in order to account for such damping effects.

With reference to a single tooth pair meshing in correspondence of the pitch point the “oil squeeze” effect in the gap has been modelled under the following tribological assumptions:

- the teeth are rigid bodies of cylindrical shape, whose axes are parallel to the gear axis. In Fig. 5 it can be noted the reference frame with the ζ axis parallel to the gear axis;
- as the radius of each cylinder it is assumed the involute radius at the pitch point;
- the cylinders approach each other in the η direction without any slip velocity in the ζ direction;
- the fluid is assumed to be incompressible with constant viscosity.

The gap height $h(\xi, t)$ between the teeth assumes than the following expression:

$$h(\xi, t) = \overline{PP'} = x(t) + \rho_1 \left[1 - \sqrt{1 - \left(\frac{\xi}{\rho_1} \right)^2} \right] + \rho_2 \left[1 - \sqrt{1 - \left(\frac{\xi}{\rho_2} \right)^2} \right], \quad (7)$$

in witch, $x(t)$ is the instantaneous value of the minimum gap while ξ takes value in the interval (–addendum, + addendum).

So, due to the smallness of the ratio ξ/ρ , the root terms may be developed as

$$\sqrt{1 - \left(\frac{\xi}{\rho} \right)^2} \cong 1 - \frac{1}{2} \left(\frac{\xi}{\rho} \right)^2$$

and Eq. (7) can be approximated in the following:

$$h(\xi, t) = x(t) + \frac{1}{2} \xi^2 \left(\frac{1}{\rho_1} + \frac{1}{\rho_2} \right). \quad (8)$$

Defining an equivalent radius as

$$R = 2 \left(\frac{\rho_1 \rho_2}{\rho_1 + \rho_2} \right) \quad (9)$$

the gap assumes the expression:

$$h(\xi, t) = x(t) + \frac{\xi^2}{R}. \quad (10)$$

With reference to the oil pressure in the gap, following the classical mono-dimensional Reynolds approach [17], it is assumed:

$$\frac{\partial}{\partial \xi} \left(\frac{h(\xi, t)^3}{\mu} \frac{\partial p}{\partial \xi} \right) = 12 \frac{\partial h(\xi, t)}{\partial t}. \quad (11)$$

The Eq. (11), integrated with the boundary conditions:

$$\begin{cases} \xi = -a \rightarrow p = 0, \\ \xi = 0 \rightarrow \frac{\partial p}{\partial \xi} = 0, \end{cases}$$

gives

$$p(\xi, t) = 3R^3 \mu \dot{x}(t) \left[\frac{1}{(a^2 + Rx(t))^2} - \frac{1}{(\xi^2 + Rx(t))^2} \right], \quad (12)$$

in which it is assumed that the pressure diagram, symmetrical with respect to the η -axis, starts at $\xi = -a$ and ends at $\xi = +a$, with $a \leq$ addendum.

By integrating the above relation along the ξ coordinate in the range $(-a, +a)$, an analytical expression for the oil squeeze force $\dot{x}S$, can be obtained:

$$\dot{x}S(x) = -3\dot{x}R^{3/2}\mu Z \frac{\left[a(a^2 - Rx)\sqrt{Rx} + (a^2 + Rx)^2 \arctan\left(\frac{a}{\sqrt{Rx}}\right) \right]}{x^{3/2}(a^2 + Rx)^2} \quad (13)$$

in which Z indicates the axial width of the gear pair, a denotes the semi-length along the the ξ direction of the oil film and is related to the lubrication conditions.

The x and \dot{x} terms in Eq. (13) are related to $\Delta\vartheta$ and $\Delta\dot{\vartheta}$ in Eq. (5) by the relations:

$$x = \Delta\vartheta_i r_{is} \quad \text{and} \quad \dot{x} = \Delta\dot{\vartheta}_i r_{is}.$$

7. Numerical simulations

The theoretical model previously described has been implemented in a Matlab-Simulink code in order to evaluate the dynamic behaviour of the system varying all the parameters that characterize the dissipative terms.

Regarding the values of the physical system parameters the reference is in Table 1.

In particular the damping value σ_t has been fixed to 1/1000 of the critical value of the subsystem (I_{1P} ; K_t ; I_{2P}).

The engine torque law has been obtained starting from the pressure cycle experimentally acquired on a 1900 cm³ four strokes and four cylinder diesel engine, under idling operating conditions at the speed of 750 rev/min.

The drag torques T_{b1} and T_{b2} was calculated by means of analytical formulas available in literature [18] being functions of the dimensions of the bearings, of the average rotating velocity and of the oil viscosity.

The teeth of the two gear pairs (first and second gear), are characterized by the given data reported in Table 2.

For the considered two-stage clutch the parameters reported in Table 3 have been adopted.

The characteristics of the oil and the lubrication mechanism are detailed in Table 4.

Table 1
System parameters

I_f (kg m ²)	Flywheel Moment of Inertia	0.1
I_{1P} (kg m ²)	First speed driving gear Moment of Inertia	1.38e ⁻⁵
I_{1S} (kg m ²)	First speed driven gear Moment of Inertia	1.36e ⁻³
I_{2P} (kg m ²)	Second speed driving gear Moment of Inertia	5.08e ⁻⁵
I_{2S} (kg m ²)	Second speed driven gear Moment of Inertia	8.49e ⁻⁴
K_t (N m)	Torsional Stiffness of the shaft between the first and the second driving gears	2.50e ⁴
σ_t (N m s)	Torsional Damping of the shaft between the first and the second driving gears	0.31

Table 2
Gear pairs data

Gear	1st speed		2nd speed	
	(driving)	(driven)	(driving)	(driven)
Number of tooth	11	43	19	41
Face width (mm)	17	13.8	13.5	12.8
Pitch radius (mm)	13.24	51.76	20.58	44.42
Module		2.41		2.17
Addendum (mm)		2.41		2.17
Tooth height (mm)		5.42		4.88
Pressure angle (deg)		24		17.5
Helix angle (deg)		23.5		32.25
Transverse contact ratio (ϵ_x)		1.43		1.75
Total contact ratio (ϵ)		2.23		2.93
Transmission ratio		3.909		2.158
Backlash (mm)			0.08	

Table 3
Clutch parameters

K_{c1} (N m/deg)	First stage Stiffness	0.087
K_{c2} (N m/deg)	Second stage Stiffness	61.0
ϕ (deg)	Transition angle between first and second stage	2
H_1 (N m)	First stage Hysteresis parameter	0.0, 0.05, 0.1, 0.15, 0.2
H_2 (N m)	Second stage Hysteresis parameter	0, 0.1, 1.0, 10.0, 20.0

Table 4
Lubrication parameters

μ (Pa s)	Absolute oil viscosity	0.004, 0.02
a_1 (m)	Oil gap extension between the teeth of the first gear	$0.01e^{-3}$, $3.0e^{-3}$
a_2 (m)	Oil gap extension between the teeth of the second gear	$0.01e^{-3}$, $3.0e^{-3}$
h_{\min} (m)	Minimum film thickness (the same for the two gear pairs)	$1.0e^{-6}$

The Matlab solver used for the numerical integration is a variable step Runge–Kutta 4,5 method (Dormand–Prince pair). The time histories sampled at 10 kHz with the relative FFT spectra and rms value have been analysed to evaluate the influence of the dissipative terms on the system dynamical behaviour.

8. Results

In order to evaluate the rattle level, the following index has been assumed:

$$(G.I.)_i = \frac{(\Delta \ddot{\vartheta}_i)_{\text{rms}}}{(\ddot{\vartheta}_f)_{\text{rms}}}, \quad i = 1, 2.$$

The above index is given by the ratio between the rms value of the relative acceleration of the generic pair and that of the flywheel.

In Fig. 6, for every gear pair, the above index versus the value of the H_1 parameter, for fixed values of the H_2 parameter, has been reported, for two different lubrication conditions. In the same figure, the table reassumes the picture of the conducted simulations.

Analysing the diagrams the following observations can be made:

Apart from a few exceptions, probably of a numerical nature,

- the value of the G.I. for the second gear is always greater than the first one;
- for the same values of the H_2 parameter, increasing the value of the H_1 parameter a G.I. reduction is observed;
- for the same values of the H_1 parameter, increasing the value of the H_2 parameter firstly a reduction and subsequently an increase of the G.I. value is noted;
- the presence of oil lubricant between the tooth always decreases the value of the G.I.

As an example the time histories of the tooth relative motion for the two gear pairs in four particular cases have been reported. The first two cases (Figs. 7 and 8) refer to the absence of hysteresis in the clutch under two different conditions: starved and full lubrication.

The second two cases (Figs. 9 and 10) refer to the pair of values of the clutch hysteresis parameters that gives the minimum value for the G.I., always in the two different lubrication conditions.

In the diagrams of the previous figures, the teeth backlash ($80 \mu\text{m}$) is covered alternatively so as to realise the contact between the flanks of the tooth in the two following different configurations: when the relative displacement is equal to $-40 \mu\text{m}$, the contact happens between the flanks of the tooth of the two gears working just in the correct way (normally loaded sides: the driving gear pushes the driven gear), when the relative displacement is equal to $+40 \mu\text{m}$, instead, the contact happens between the flanks assigned, in normal conditions, to not work (normally unloaded sides: the driven gear pushes the driving gear).

This situation of impacts on both flanks of the teeth is defined in literature as double side impact. Moreover, due to the elastic compliance of the teeth, values of the relative displacement greater, in module, than $40 \mu\text{m}$, are possible.

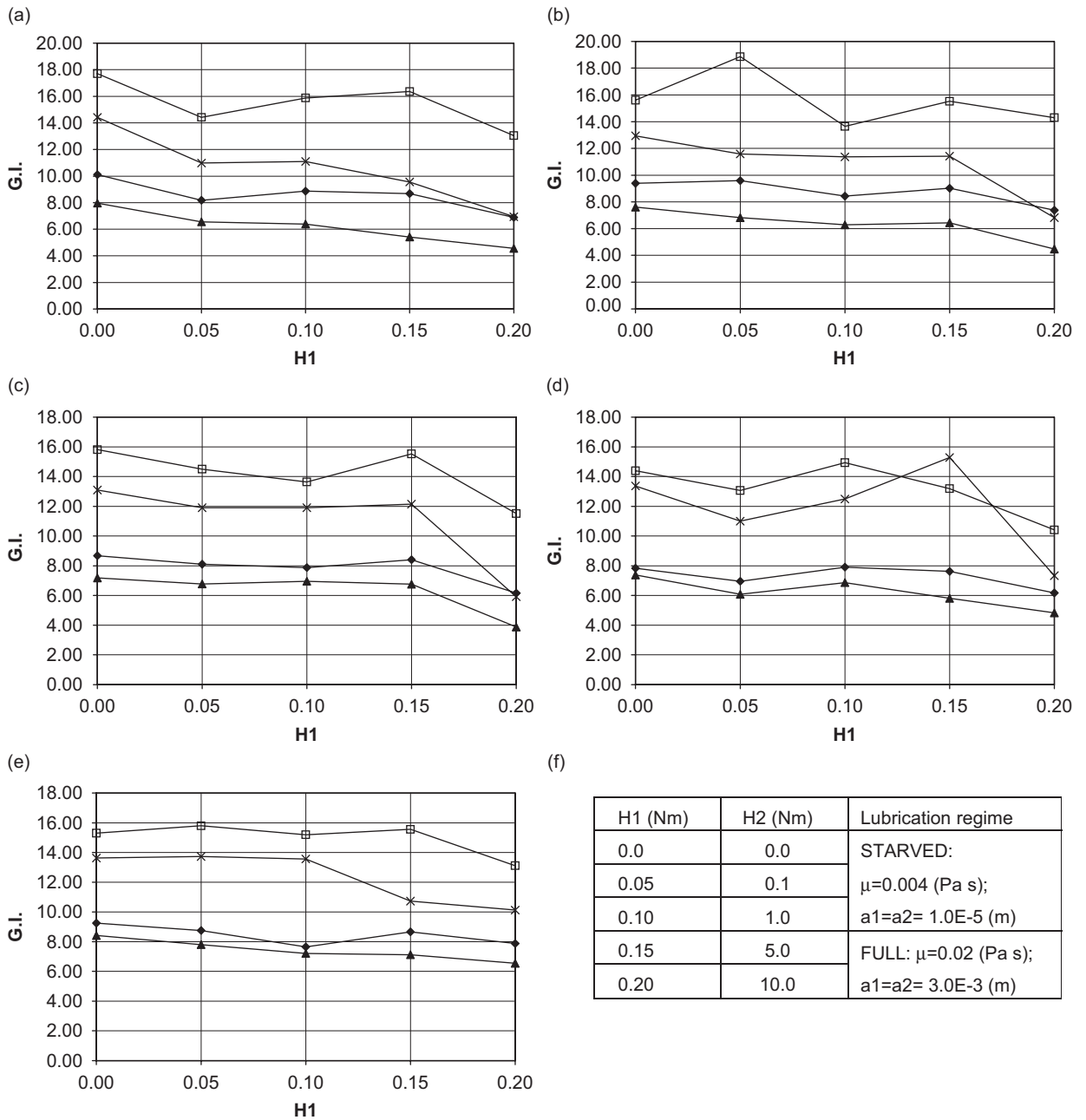


Fig. 6. Simulation results: gear index vs. H_1 for: (a) $H_2 = 0.0$, (b) $H_2 = 0.1$, (c) $H_2 = 1.0$, (d) $H_2 = 5.0$, (e) $H_2 = 10.0$, and (f) prospect of the numerical experimentation. \blacklozenge first gear, starved lubrication; \square second gear, starved lubrication; \blacktriangle first gear, full lubrication; \times second gear, full lubrication.

The comparison between the time histories permits the following considerations:

The presence of the oil, besides reducing the total number of impacts between the tooth, reduces also their intensity as it can be noted from the amplitude of the elastic deformation consequent to the collision. Thanks to the squeeze effect, in fact, the oil reduces the tooth speed in the phase of gap crossing.

The contribution given by the terms of the clutch hysteresis in the rattle reduction is evident by comparison between the Figs. 7 and 9 both relative to a starved lubrication regime. in Fig. 9, in fact, it can be noted the

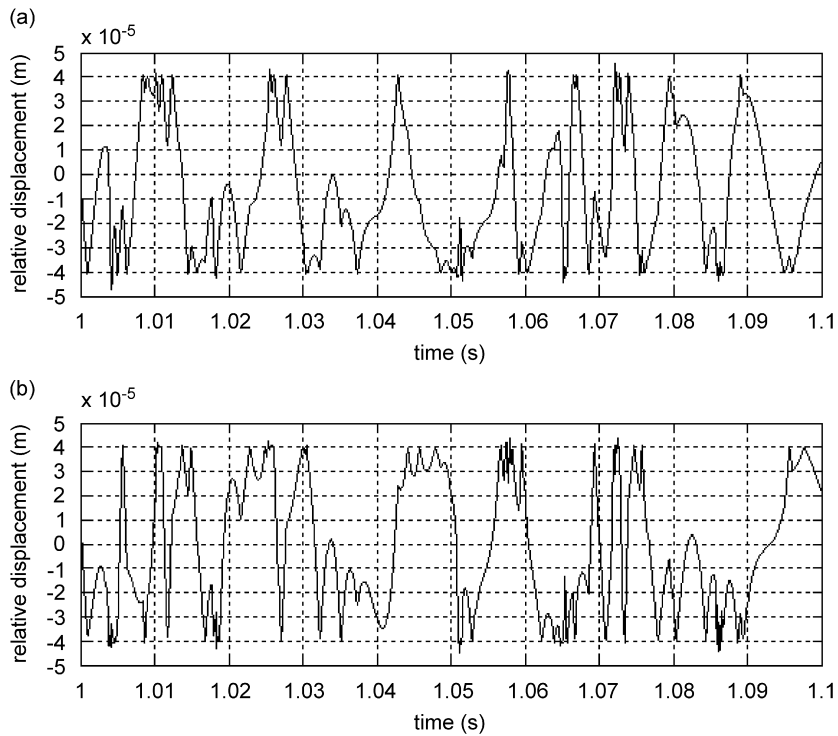


Fig. 7. Time histories of the relative motion between the teeth of the (a) first and the (b) second gear pairs. $H_1 = 0.0$, $H_2 = 0.0$, starved lubrication. $G.I._1 = 10.1$, $G.I._2 = 17.7$.

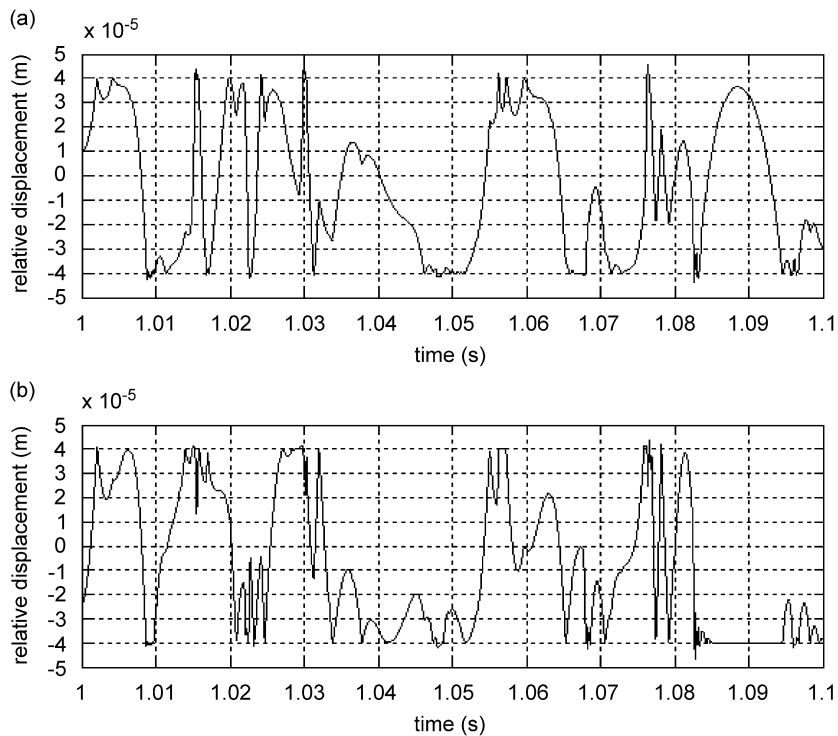


Fig. 8. Time histories of the relative motion between the teeth of the (a) first and the (b) second gear pairs. $H_1 = 0.0$, $H_2 = 0.0$, full lubrication. $G.I._1 = 8.0$, $G.I._2 = 14.4$.

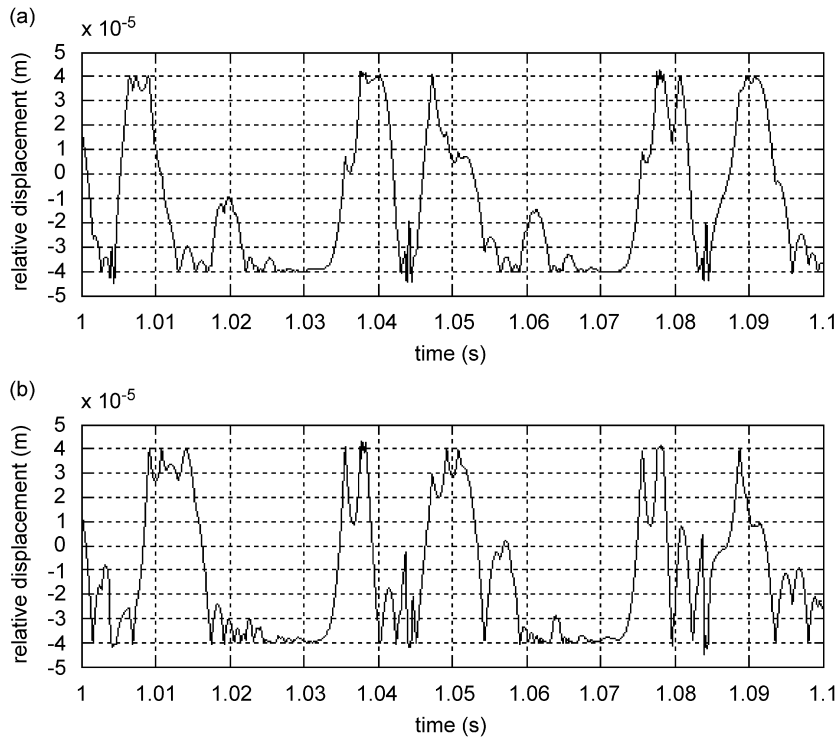


Fig. 9. Time histories of the relative motion between the teeth of the (a) first and the (b) second gear pairs. $H_1 = 0.2$, $H_2 = 1.0$, starved lubrication. $G.I._1 = 6.2$, $G.I._2 = 11.5$.

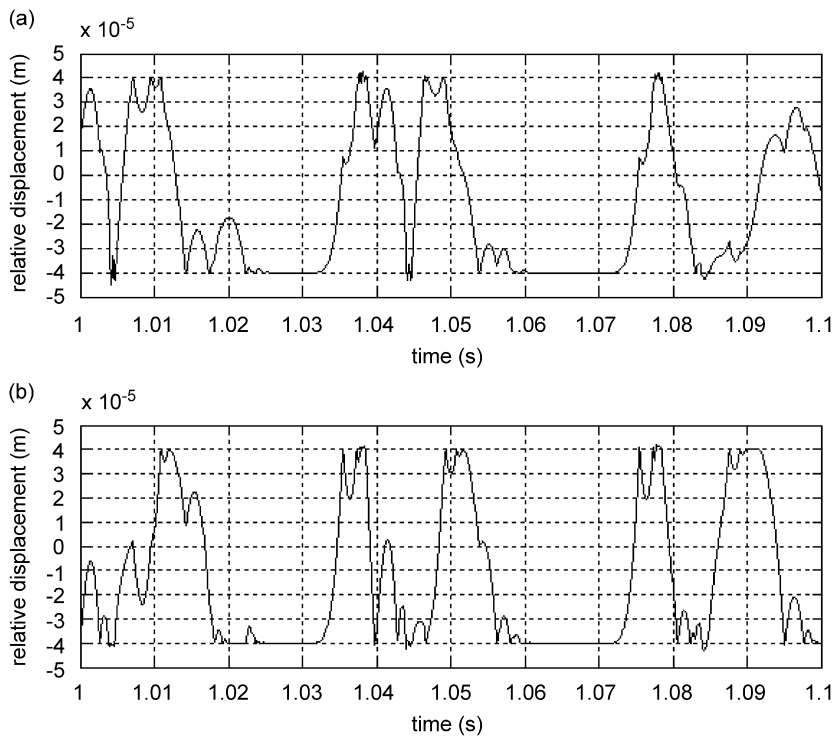


Fig. 10. Time histories of the relative motion between the teeth of the (a) first and the (b) second gear pairs. $H_1 = 0.2$, $H_2 = 1.0$, full lubrication. $G.I._1 = 3.9$, $G.I._2 = 5.9$.

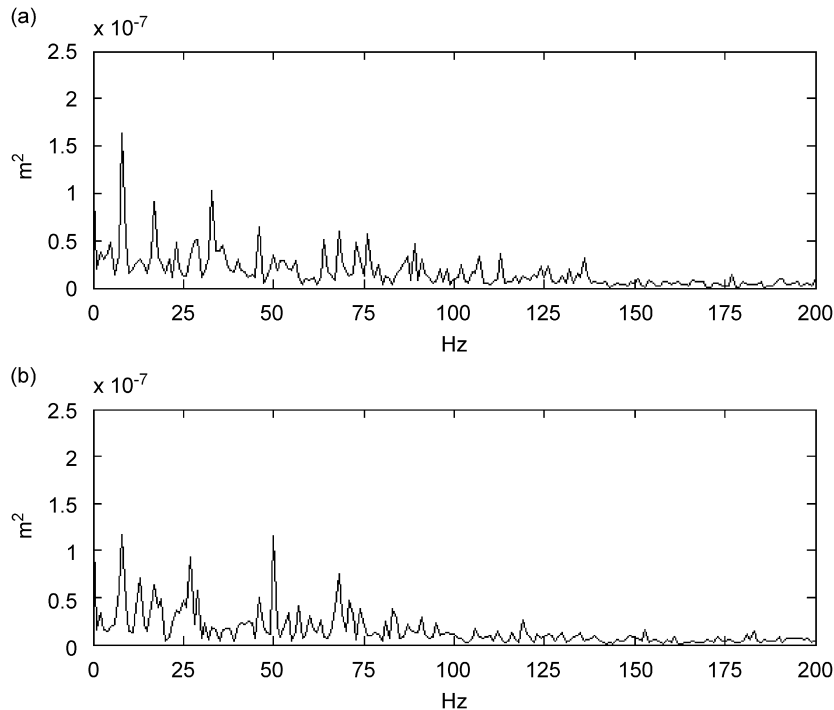


Fig. 11. Power density spectra of the relative motion between the teeth of the (a) first and the (b) second gear pairs. $H_1 = 0.0$, $H_2 = 0.0$, starved lubrication. $G.I._1 = 10.1$, $G.I._2 = 17.7$.

presence of sporadic impacts on the normally unloaded flanks and a relatively wide contact phase between the normally loaded ones. Finally, comparing Fig. 9 with Fig. 10 a further rattle reduction, due to a full lubrication, can be observed.

The Power Spectra conducted on the relative motion signals relative to a period of 1 second of simulation after a suitable transient, can be of assistance in the interpretation of the different dynamic behaviours.

Figs. 11 and 12 refer to the case of null values for the hysteresis clutch parameters H_1 and H_2 in two different lubrication regimes: “Starved” and “Full and Cold”, this last lubrication regime is characterized by a full meatus extension and a value of the viscosity ($\mu = 0.5 \text{ Pa s}$) typical of a gear box oil during the warm-up transient.

In the case of starved lubrication (Fig. 11), there is the presence of many frequency components denoting a dynamic behaviour characterized by several “double sided” impacts and rebounds.

In contrast, in the “full lubrication” case (Fig. 12) the Power spectrum shows, in a more evident manner, the presence of a great 50 Hz frequency component (twice the excitation fundamental frequency), describing hence a dynamic behaviour more regular with regard to the vibro-impacts and, then, a more favourable operating condition with respect to the gear rattle phenomenon.

9. Conclusions

The developed driveline model made it possible to conduct an analysis concerning the effects exerted by the dissipative terms, due to the clutch and the oil lubricant, on the “idle” gear rattle phenomenon.

The obtained results enabled a qualitative and, in part, also quantitative evaluation of the contribution of the above mentioned two elements in reducing the phenomenon under examination.

The effects due to the clutch, as known in literature, essentially consist in an action of mechanical filtering on the forces that determine rattle vibration.

Instead, the effect of impacts attenuation due to the oil film, in the authors’ knowledge, is neglected in the driveline models even though supplying, as evidenced by the conducted simulations, a contribution to the rattle reduction, that can be, in some cases, comparable with that due to the clutch hysteresis.

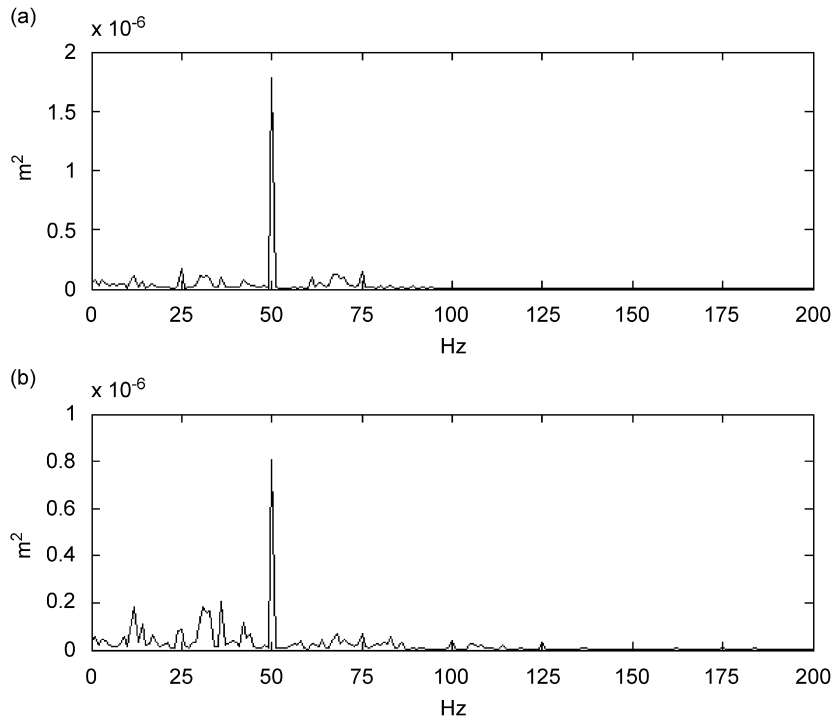


Fig. 12. Power density spectra of the relative motion between the teeth of the (a) first and the (b) second gear pairs. $H_1 = 0.0$, $H_2 = 0.0$, full lubrication, $\mu = 0.5 \text{ Pa s}$. $G.I._1 = 5.51$, $G.I._2 = 6.20$.

In the opinion of the authors, finally, a greater effort should be made by gear rattle researchers in the definition of an index of rattle that better relates the vibrations and the impacts with the produced noise.

From the analysis of the presented results in fact, it seems evident that not all the impacts happen with the same violence and therefore their contribution to noise, and also to wear, differs considerably.

New experimental studies together with theoretical analyses should have therefore, among their goals, a definition of a more objective index for the quantification of gear rattle phenomenon.

References

- [1] R. Singh, H. Xie, R.J. Comparin, Analysis of automotive neutral gear rattle, *Journal of Sound and Vibration* 131 (2) (1989) 177–196.
- [2] C. Padmanabhan, T.E. Rook, R. Singh, Modeling of automotive gear rattle phenomenon: state of the art, SAE Paper no. 951316, 1995.
- [3] C.L. Gaillard, R. Singh, Dynamic analysis of automotive clutch dampers, *Applied Acoustics* 60 (2000) 399–424.
- [4] Y. Wang, R. Manoj, W.J. Zhao, Gear rattle modeling and analysis for automotive manual transmissions, *Proceedings of IMech, Journal of Automobile Engineering* 215 (part D) (2001) 241–258.
- [5] T.C. Kim, R. Singh, Dynamic interactions between loaded and unloaded gear pairs under rattle conditions, SAE Paper 2001-01-1553, 2001.
- [6] C. Padmanabhan, R.C. Barlow, T.E. Rook, R. Singh, Computational issues associated with gear rattle analysis, *ASME Journal of Mechanical Design* 117 (1995) 185–192.
- [7] W. Reik, R. The dual mass flywheel, 6th Luk Symposium 1998.
- [8] S. Meisner, B. Campbell, Development of gear rattle analytical simulation methodology, SAE Paper 951317, 1995.
- [9] Y. Wang, Modelling and analysis of automotive transmission rattle, SAE Paper 972054, 1997.
- [10] C. Delprete, C. Rosso, Numerical analysis of gear rattle, SAE Paper 2005-01-1786, 2005.
- [11] A. Forcelli, T. Pappalardo, C. Grasso, A new approach for objective measurements of transmission gear rattle noise, 2004 JSAE Annual Congress, Yokohama, Japan, 2004.
- [12] F. Sbarbati, C. Grasso, M. Martorelli, P. Liccardo, L. Tosato, M. Uberti, M. Malusardi, Gear rattle optimisation, FISITA 2004, World Automotive Congress, Barcelona, Spain, 2004.
- [13] S.N. Dogan, Loose part vibration in vehicle transmissions gear rattle, *Turkish Journal of Engineering and Environmental Science* 23 (1999) 439–454.

- [14] R. Brancati, E. Rocca, R. Russo, A gear rattle model accounting for oil squeeze between the meshing gear teeth, *Proceedings of the Institution of Mechanical Engineers, Part D, Journal of Automobile Engineering* 219 (9) (2005) 1075–1083.
- [15] K. Umezawa, T. Suzuki, T. Sato, Vibration of power transmission helical gears (approximate equation of tooth stiffness), *Bulletin of JSME* 29 (251) (1986) 1605–1611.
- [16] Y. Cai, Simulation on the rotational vibration of helical gears in consideration of the tooth separation phenomenon (a new stiffness function of helical involute tooth pair), *Transactions of ASME, Journal of Mechanical Design* 117 (1995) 460–469.
- [17] A.Z. Szeri, *Tribology: Friction, Lubrication and Wear*, McGraw-Hill, New York, 1980.
- [18] SKF—Bearing Handbook.